Selective nuclear-spin interaction based on a dissipatively stabilized nitrogen-vacancy center

Jiawen Jiang and Q. Chen*

Department of Physics and Key Laboratory of Low Dimensional Quantum Structures and Quantum Control of Ministry of Education, Hunan Normal University, Changsha 410081, China

(Received 24 October 2021; accepted 1 April 2022; published 15 April 2022)

Current typical methods to realize nuclear-nuclear quantum gates require a sequence of electron-nuclear quantum gates by using dynamical decoupling techniques, which are implemented at low temperature because of the short decoherence and relaxation time of the nitrogen-vacancy (NV) spin at room temperature. This limitation could be overcome by using periodic resets of an NV spin as a mediator of the interaction between two nuclear spins [Q. Chen *et al.*, Phys. Rev. Lett. **119**, 010801 (2017)]. However, this method works under stringent coupling strength conditions, which makes it not applicable to heteronuclear quantum gate operations. Here we develop this scheme by using radio-frequency fields to control different nuclear-spin species. Periodic resets of the NV center protect the nuclear spins from decoherence and relaxation of the NV spin. Radio-frequency control provides the probability to have highly selective and high-fidelity quantum gates between heteronuclear spins and detecting nuclear spins by using a nuclear-spin sensor under ambient conditions.

DOI: 10.1103/PhysRevA.105.042426

I. INTRODUCTION

Nuclear spins in materials such as diamond associated with single defects represent a promising platform for quantum information registers [1–4] and sensing purposes [5–13] due to their long coherence times and the potentially large number of available spins. Nuclear spins can be initialized, controlled, and read out through the electron spin of the nitrogen-vacancy (NV) center [14] driven by optical fields and microwave radiation [15,16]. Recent progress manifests in a number of works, such as electron-nuclear [17–26], electron-electron [27], and nuclear-nuclear quantum gates [28]. Many schemes are proposed to realize electron-nuclear quantum gate operations, both with [23,24] and without [25,26] additional radio-frequency (rf) control of the nuclear spins themselves.

A nuclear-nuclear quantum gate is implemented by a sequence of NV nuclear quantum operations [1,2]; it is a delicate issue to have a complete set of quantum gates on specific nuclei in samples [23]. Current related experiments are operated at low temperature, because of the relatively short lifetime of the NV center. Several outstanding challenges are caused by the relaxation and decoherence processes of the electron spin as these limit quantum gate fidelities on nuclear registers as well as spectral resolution and selectivity. A scheme was proposed to have highly selective and high-fidelity quantum gates between nuclear spins under ambient conditions [29]. However, it has strict requirements of resonance conditions and is applicable for special cases, i.e., for nuclear spins in the same species with the parallel coupling components between the NV and nuclear spins far smaller than the vertical components.

Here we extend the scheme in Ref. [29] to a heteronuclear case by using radio-frequency fields to control different nuclear-spin species individually. The consideration of different species might be inevitable for some specific purposes, such as sensing and quantum information processing of molecular spins [30]. Our method not only is general for quantum computing made of NV-controlled nuclei in and out of the diamond lattice [31], but also could be applied to control ^{13}C and ^{29}Si spins with silicon vacancies in silicon carbide [32]. The effective substantial second-order coupling between the nuclear spins is obtained through a microwave (MW) driving NV center which is periodically reinitialized by a dissipative process [29]. Similarly, the periodic reinitialization of the NV center decouples it from the dynamics and its effect on the system is an effective weak dissipation process. Thus the high selectivity and fidelity of the nuclear-spin quantum gate for different nuclear-spin species could be possible even at ambient conditions, which is an extension of quantum computation and simulation applications by using different nuclear species controlled by NV centers. Additionally, one can use a nuclear spin as a quantum sensor to detect nuclear spins in another species as well as analysis of complex spin structures.

This paper is structured as follows. We start with the derivation of the effective Hamiltonian of the system by using Schrieffer-Wolf transformation [33,34], which demonstrates the validity of the indirect interaction between nuclear spins by the application of suitably tuned rf fields. We take two relevant species, i.e., ^{13}C and ^{29}Si spins, as examples to show our protocol efficiency. Coherent evolution between a ^{13}C and a ^{29}Si spin is limited by the NV lifetime; this limitation is overcome through periodic resets of NV spin. The feasibility of high-selectivity and -fidelity nuclear-nuclear quantum gates by using rf controls is discussed as well as the sensing application. Finally, we compare our approach to the previous scheme in Ref. [29].

*qchen@hunnu.edu.cn

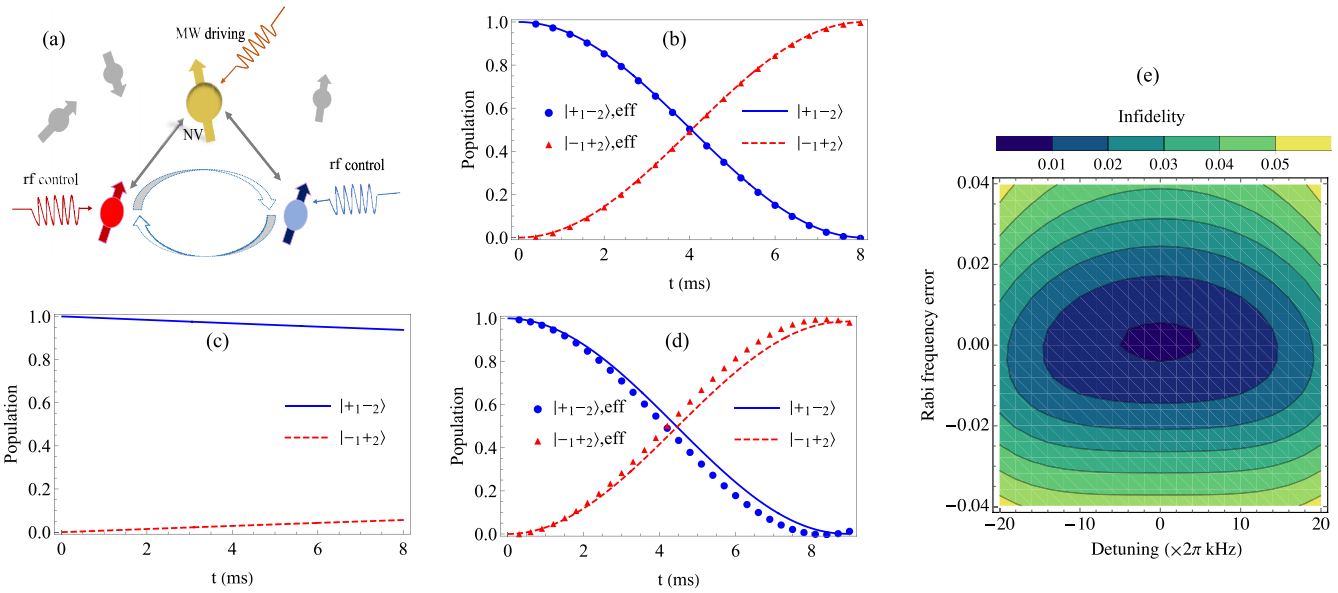

FIG. 1. (a) The NV center mediates the coupling between the first spin (^{13}C) with $\gamma_{n1}B = 2\pi \times 6.40$ MHz and the second spin (^{29}Si) with $\gamma_{n2}B = 2\pi \times 5.06$ MHz to achieve a quantum gate, while itself is decoupled from the dynamics. Radio-frequency fields are applied to control two nuclear-spin species individually, when we use a continual MW field to drive the NV spin. (b) Population evolutions are shown by considering the ideal case in which no dissipation is included and the nuclear spins are initialized in the state $|+_1 -_2\rangle$. The Rabi frequencies of rf fields are given by $\Omega_{\text{rf1}} = \Omega_{\text{rf2}} = 2\pi \times 1$ kHz, microwave driving field $\Omega = 2\pi \times 400$ kHz, the parallel coupling components $[a_{\parallel 1}, a_{\parallel 2}] = 2\pi \times (9, 11)$ kHz, and the effective coupling coefficient $g_e = 2\pi \times 0.12$ kHz. These exact numerical simulations using Eq. (5) fit well with the theoretical derivation of the effective (eff) dynamics under the Hamiltonian (7). (c) Considering the practical case and using the same parameters as in (b) with the NV dissipation included as $T_{1\rho} = 200$ μs, exact numerical simulation of the master equation (10) shows that there is no coherent evolution between the nuclear spins due to the NV lifetime limitation. (d) The periodic NV reset makes it possible to extend the coherent evolution of the heteronuclear spins well beyond the NV spin lifetime. The exact numerical calculation is based on Eq. (17), when we simulate the effective master equation (14) of nuclear spins. The parameters are the same as in (b) except that the NV center is reinitialized to the state $|-\rangle_e$ every $t_{\text{re}} = 20$ μs. (e) Process infidelity for different detuning and errors of the MW driving of the NV center.

II. INDIRECT INTERACTION BETWEEN NUCLEAR SPINS

We consider two nuclear spins in different species coupled to an electron spin of a single NV center. An MW field and an rf field are used for external control over the electron and nuclear spins as well as for achieving selective internuclear interactions [see Fig. 1(a)]. The magnetic field B is applied along the NV axis (the $\hat{z}$ axis), which is large enough to split the degenerate states of $|m_s = |\pm 1\rangle$. The Hamiltonian of the whole system is given by

$$H = DS_z^2 + \gamma_e B S_z + \sum_i \gamma_{ni} B I_i^z + S_z \sum_i \vec{A}_i \cdot \vec{I}_i + H_w + H_r. \quad (1)$$

Note that we hereafter omit the Dirac constant $\hbar$ for simplicity. Here $D = 2\pi \times 2.87$ GHz denotes the zero-field splitting of the electronic ground state and γ_e and γ_{n_i} are the gyromagenetic ratios of the electron spins and nuclear spins, respectively. The interaction between the NV center and the ith nucleus is mediated by the hyperfine vector $\vec{A}_i$, where $A_i = (a_{\parallel i}, a_{\perp i})$, with $a_{\parallel i}$ and $a_{\perp i}$ denoting the related coupling components parallel and perpendicular to the nuclear-spin quantization axes $a_{\parallel i} = \vec{A}_i \cdot \hat{z}$ and $a_{\perp i} = \sqrt{|\vec{A}_i|^2 - a_{\parallel i}^2}$, respectively. The Hamiltonians H_w and H_r describe the action of the MW driving and rf fields, respectively, which read

$$H_w = \sqrt{2}\Omega \cos \omega t S_x, \quad (2)$$

$$H_r = \sum_i 2\Omega_{\text{rf}i} \cos \omega_{\text{rf}i} t I_i^x, \quad (3)$$

where Ω ($\Omega_{\text{rf}i}$) is the Rabi frequency of the MW (rf) driving field with the corresponding frequency ω ($\omega_{\text{rf}i}$).

The MW driving field is applied to be on resonance with the transition $|-1\rangle \leftrightarrow |0\rangle$ as $\omega = D - \gamma_e B$. We can rewrite the effective Hamiltonian of the NV center as $H_{\text{NV}} = \Omega\sigma_z$. Then in the rotating frame with $H_0 = (D - \gamma_e B)|-1\rangle\langle -1|$, the Hamiltonian could be rewritten as

$$H_t = \Omega\sigma_z + \sum_i \left(\gamma_{ni} B + \frac{a_{\parallel i}}{2}\right) I_i^z + a_{\parallel i}\sigma_x I_i^z + a_{\perp i}\sigma_x I_i^x + H_r, \quad (4)$$

where $\sigma_z = \frac{1}{2}(|+\rangle_e\langle +| - |-\rangle_e\langle -|)$, with $|+\rangle_e = \frac{1}{\sqrt{2}}(|0\rangle + |-1\rangle)$ and $|-\rangle_e = \frac{1}{\sqrt{2}}(|0\rangle - |-1\rangle)$.

Two weak rf fields are applied to individually control two different nuclear spins with $\omega_{\text{rf}i} = \gamma_{ni} B + \frac{a_{\parallel i}}{2}$. Working in the rotating frame with $H_0' = \sum_i (\gamma_{ni} B + \frac{a_{\parallel i}}{2}) I_i^z$ and by assuming $a_{\parallel i}, a_{\perp i} \ll \Omega \ll \omega_{\text{rf}i}$ and that $a_{\parallel i}$ is comparable to or larger than $a_{\perp i}$, the total Hamiltonian of the system can be

approximated as

$$H_t' = \Omega\sigma_z + \sum_i \Omega_{\mathrm{rf}i} I_i^x + a_{\|i}\sigma_x I_i^z. \tag{5}$$

Consider the Hamiltonian of the form $H_t' = H_{\mathrm{NV}}' + V$, where $H_{\mathrm{NV}}' = \Omega\sigma_z$ is the Hamiltonian of the MW driving and $V = \sum_i \Omega_{\mathrm{rf}i} I_i^x + a_{\|i}\sigma_x I_i^z$ is the weak perturbation with $a_{\|i}, \Omega_{rfi} \ll \Omega$. By using the Schrieffer-Wolff transformation [33,34] in condensed matter, the second-order expansion due to perturbation terms V can be obtained as

$$\langle\alpha|H_e|\beta\rangle_e = \frac{1}{2}\sum_i \left(\frac{\langle\alpha|V|i\rangle\langle i|V|\beta\rangle_e}{E_\alpha - E_i} - \frac{\langle\alpha|V|i\rangle\langle i|V|\beta\rangle_e}{E_i - E_\beta} \right), \tag{6}$$

in which $\alpha, \beta, i = \{+, -\}$, H_e is defined as the effective Hamiltonian of the system, and E_k ($k = \{+, -\}$) is the energy corresponding to the state $|k\rangle_e$. By simple calculations, we find $\langle +|H_e|+\rangle_e = g_e I_1^z I_2^z$, in which $|i\rangle_e = |-\rangle_e$ is the channel state of the virtual electron spin flip, when $\langle -|H_e|-\rangle_e = -\langle +|H_e|+\rangle_e = g_e I_1^z I_2^z$ with the channel state $|i\rangle_e = |+\rangle_e$, here $g_e \approx \frac{a_{\|1}a_{\|2}}{2\Omega}$. Thus we adiabatically eliminate the fast electronic degrees of freedom from the slow nuclear dynamics by a Schrieffer-Wolff (SW) transformation and derive the effective Hamiltonian

$$H_e \approx \sum_{i=1,2} \Omega_{\mathrm{rf}i} I_i^x + g_e I_1^z I_2^z \otimes (|+\rangle_e\langle +| - |-\rangle_e\langle -|). \tag{7}$$

Typically, the environmental noise of the NV center is dominated by its nearby nuclear spins, which fits the Markovian approximation [35,36]. To investigate the dynamics of the whole system described by the density matrix ρ, the system is governed by the master equation

$$\frac{d\rho}{dt} = -i[H_t', \rho] + L_e\rho L_e^\dagger - \frac{1}{2}(L_e L_e^\dagger \rho + \rho L_e L_e^\dagger) \tag{8}$$

in which $L_e = \sqrt{\gamma_e}|-\rangle_e\langle +|$ with $\gamma_e = 1/T_{1\rho}$. We apply this method and evaluate the performance of the gate between the first spin (^{13}C) with $\gamma_{n1}B = 2\pi \times 6.40$ MHz and the second spin (^{29}Si) with $\gamma_{n2}B = 2\pi \times 5.06$ MHz coupled to an NV center with $(a_{\|1}, a_{\|2}) = 2\pi \times (9, 11)$ kHz [see Fig. 1(a)]. Here the driving fields are given as rf Rabi frequencies $\Omega_{\mathrm{rf}1} = \Omega_{\mathrm{rf}2} = 2\pi \times 1$ kHz, and the MW Rabi frequency $\Omega = 2\pi \times 400$ kHz. Note that in our scheme, we neglect the effect of rf fields on the NV center, because the rf driving detunings are more than three orders higher than the Rabi frequencies. The NV center is initialized to the state $|-\rangle_e$, when the nuclear spins are initialized to $|+_1\, -_2\rangle$ with $|+_i\rangle = \frac{1}{2}(|\uparrow_i\rangle + |\downarrow_i\rangle)$. Perfect state transfer between nuclear spins ^{29}Si and ^{13}C $|+_1\, -_2\rangle \to |-_1\, +_2\rangle$ is shown in Fig. 1(b), in which the population evolutions from using the effective second-order Hamiltonian (7) fit well with the exact total Hamiltonian of the system (5). The effective Hamiltonian (7) includes a three-body interaction and there are two channels that can mediate the internuclear interaction via virtual electron spin flips through the NV microwave dressed states $|+\rangle_e$ and $|-\rangle_e$. However, the two channels can be mixed up if the nuclear-nuclear interaction time is longer than the NV relaxation time. As shown in Fig. 1(c), in the case when the lifetime of the NV center $T_{1\rho} = 200$ μs, there is no coherent evolution of the nuclear spins. Therefore, the system is limited by the NV relaxation at room temperature.

III. EFFECT OF ELECTRON-SPIN RESETS

In our scheme, in order to overcome the limitation of NV relaxation, we intend to periodically reset the electron spin to the state $|-\rangle_e$ within its relaxation time $T_{1\rho}$. It is reasonable to consider the steady-state polarization of the NV spin in a quasisteady state as

$$\langle 2\sigma_z\rangle = e^{-t_{\mathrm{re}}/T_{1\rho}} = p. \tag{9}$$

The three-body interaction in the effective Hamiltonian (7) can be estimated as $g_e I_1^z I_2^z \otimes (|+\rangle_e\langle +| - |-\rangle_e\langle -|) \approx g_e I_1^z I_2^z \langle 2\sigma_z\rangle = p g_e I_1^z I_2^z$. Therefore, the NV spin is not involved in the nuclear-nuclear interaction Hamiltonian. Resets also introduce another dissipation item in the master equation and it is reasonable to have the effective relaxation of the NV spin as $\gamma_r = 1/T_{1\rho} + 1/t_{\mathrm{re}}$. Thus, we can rewrite the master equation of the system as

$$\frac{d\rho}{dt} = -i[H_t', \rho] + L_r\rho L_r^\dagger - \frac{1}{2}(L_r^\dagger L_r\rho + \rho L_r^\dagger L_r), \tag{10}$$

in which $L_r = \sqrt{\gamma_r}|-\rangle_e\langle +|$. The non-Hermitian Hamiltonian of the quantum jump formalism [37] of the NV spin is given by

$$H_H = \Omega\sigma_z - \tfrac{1}{2}L_r^\dagger L_r. \tag{11}$$

According to the second expansion of the SW transformation, we have an energy difference between $|+\rangle_e$ and $|-\rangle_e$ as a complex energy $E_+ - E_- = \Omega - \frac{i}{2}\gamma_r$. We can derive an effective Hamiltonian

$$H_e' \approx \sum_i \Omega_{\mathrm{rf}i} I_i^x + g_e' I_1^z I_2^z \otimes (|+\rangle_e\langle +| - |-\rangle_e\langle -|), \tag{12}$$

$$L_n \approx \sum_k \frac{\sqrt{\gamma_r}a_{\|k}}{\Omega - \frac{i}{2}\gamma_r} I_k^z \otimes (|+\rangle_e\langle +| - |-\rangle_e\langle -|), \tag{13}$$

in which the effective dissipation item is given by $\langle\alpha|L_e|\beta\rangle = \sum_i \frac{\langle\alpha|L_r|i\rangle\langle i|V|\beta\rangle}{E_\alpha - E_i}$ and the effective coupling is

$$g_e' \approx \frac{\Omega a_{\|1}a_{\|2}}{2\left(\Omega^2 + \frac{\gamma_r^2}{4}\right)}.$$

With the electron spin periodically reset in the state $|-\rangle_e$ with the definition $\langle 2\sigma_z\rangle = p$, we have the effective master equation of the nuclear spins as

$$\frac{d}{dt}\rho_n = -i[H_N, \rho_n] + L_N\rho_n L_N^\dagger - \frac{1}{2}(L_N^\dagger L_N\rho_n + \rho_n L_N^\dagger L_N), \tag{14}$$

with the effective Hamiltonian and Lindblad operators

$$H_N \approx \sum_i \Omega_{\mathrm{rf}i} I_i^x + p g_e' I_1^z I_2^z, \tag{15}$$

$$L_N \approx \sum_k \frac{\sqrt{p\gamma_r}a_{\|k}}{\Omega - \frac{i}{2}\gamma_r} I_z^k. \tag{16}$$

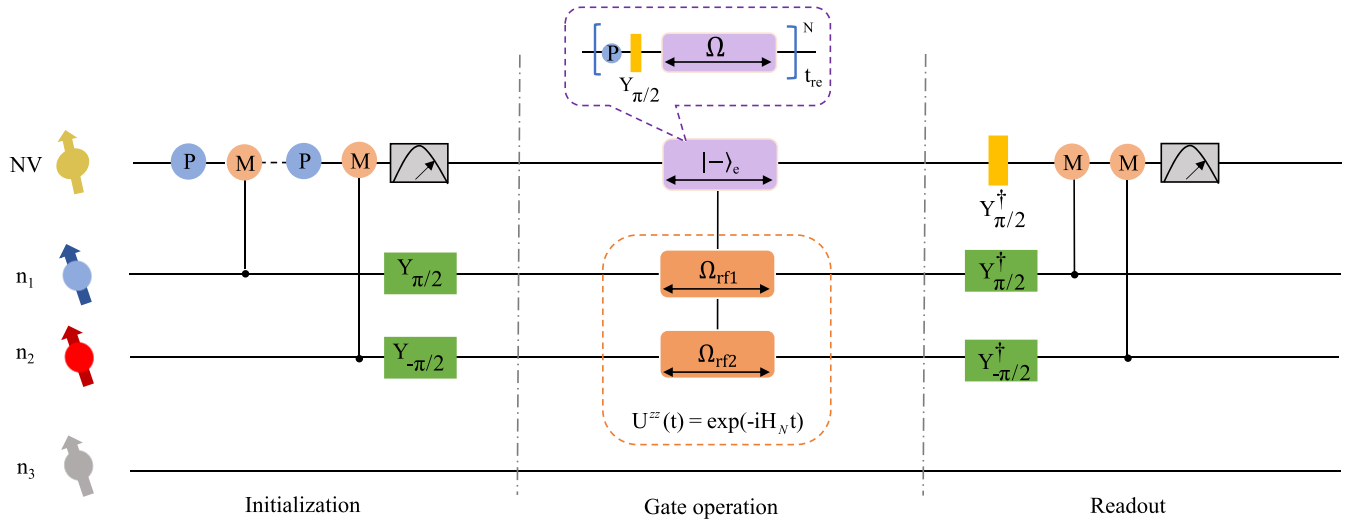

FIG. 2. Nuclear-nuclear quantum gate of two nuclear spins mediated by an NV center in diamond. The basic logic operations contain the initialization, gate operation based on second-order coupling, and readout of nuclear spins. The electron spin works as a quantum bus and is stabilized in a quasisteady state by periodically resetting in $|-\rangle_e$, which is shown in the yellow dashed box. Here P and M stand for the electron- (nuclear-)spin polarization, Y_θ represents the operation with rotation angle θ about the Y axis, and N is the total number of resets.

The effective dissipation rate is given by

$$\gamma_N = \sum_{i,j} \frac{p\gamma_r a_{\|i} a_{\|j}}{\Omega^2 + \frac{\gamma_r^2}{4}}.$$

Therefore, in principle, if the resonant conditions $\Omega_{\rm rf1} = \Omega_{\rm rf2}$ and $pg'_e \gg \gamma_N$ are satisfied, a perfect coherent state transition between the nuclear spins is possible.

For comparison, it is necessary to employ exact numerical simulations as well to show the efficiency of our theory. Exact state evolutions of the system are simulated as follows. The NV center is reinitialized periodically to the state $|-\rangle_e$ of the dressed state basis, namely, $\rho(Nt_{\rm re}) \to [{\rm Tr}_e \rho(Nt_{\rm re})] \otimes |-\rangle_e\langle -|$, where ${\rm Tr}_e$ denotes the partial trace over the electron spin and N is an integer, and the reset of the NV spin every $t_{\rm re}$ introduces an effective interaction time in each cycle. The density matrix of the system evolves according to

$$\rho_n \to \cdots U_t {\rm Tr}_e[U_t(\rho_n \otimes |-\rangle_e\langle -|)U_t^\dagger] \otimes |-\rangle_e\langle -| U_t^\dagger, \quad (17)$$

in which U_t is the time-evolution operator according to the master equation (10). Both of the state evolutions using the exact numerical simulation and effective second-order master equation based on Eqs. (17) and (14) are shown in Fig. 1(d), where the importance of periodic reinitialization of electron spin is illustrated.

We consider the same case of a ^{29}Si and a ^{13}C spin coupled to an NV spin which is presented in Sec. II except that the NV center is reinitialized to the state $|-\rangle_e$ every $t_{\rm re} = 20\ \mu$s. The resonant condition is matched as $\Omega_{\rm rf1} = \Omega_{\rm rf2} = 2\pi \times 1$ kHz and the simulations of both the exact numerical calculations and the effective master equation show perfect state transfer between the nuclear spins of ^{29}Si and ^{13}C, $|+_1 -_2\rangle \to |-_1 +_2\rangle$ [see Fig. 1(d)]. The state evolutions based on the effective master equation are slightly different from the exact simulations. The possible reason is that high orders of the SW transformation expansions are not included.

In the absence of periodic reinitialization of the electron spin, channel mixing leads to no coherent evolution of the nuclear spins [see Fig. 1(c)], while periodic reinitialization of the NV center to the state $|-\rangle_e$ provides a priority channel during the operations and it is possible for coherent evolution between the nuclear spins to extend beyond the lifetime of the NV spin. High fidelity of the nuclear-nuclear quantum gate in one step is possible (greater than 0.99), which could be significantly higher than the fidelity (less than 0.66) of nuclear-nuclear gates achieved so far with NV centers by using four electron-nuclear-spin quantum gates (if each fidelity is less than 0.90 [1]). Additionally, because of the second-order coupling, the scheme is not sensitive to the detunings from the resonance and Rabi frequency errors of the MW driving of the NV center [see Fig. 1(e)]. The process fidelity of two nuclear spins is given by the overlap of the states corresponding to the implemented evolution $|\psi\rangle = U^{zz} \otimes \sum_{i,j} |i_1\rangle|j_2\rangle/4$ $(i, j = +, -)$ to the target states.

IV. QUANTUM GATE IMPLEMENTATION

In Fig. 2 we include all the related operations of the nuclear ZZ gate implementation for experiments. The initialization consists of the electron- (nuclear-)spin polarization P (M). The electron spin of the NV center can be optically initialized and read out by using laser illumination. Here P is obtained by the optical pumping cycle available for NV centers [38,39], whereas M is based on the techniques developed for the nuclear single-shot measurement [40,41], followed by the electron state-dependent fluorescence [38,39]. Gate operation includes three steps. (i) Polarize the ^{13}C and ^{29}Si nuclear spins by using the NV center, which leads to the initial state $|-\rangle_e \otimes |+_1 -_2\rangle$ of the system. (ii) Implement the gate operation, which is governed by the effective master equation (14) $U^{ZZ}(t) = \exp(-iH_N t)$. In this process, we periodically reset the NV center and we control the heteronuclear spins via rf fields individually. (iii) Use the NV center to read out the

states of nuclear spins. Here we suppose that the ^{13}C and ^{29}Si spins can be well controlled by a SWAP gate between the NV and nuclear spin, i.e., they can be polarized and their positions can be detected precisely.

An rf field is applied to the ^{13}C sensor resonantly when the frequency of the other rf field is swept and $\gamma_{n2}B = 2\pi \times 5.06$ MHz. Assuming that $\delta_2 = \gamma_{n2}B + \frac{a_{\|2}}{2} - \omega_{\rm rf2}$ is a detuning from the resonance of rf driving to the ^{29}Si spin, the effective Hamiltonian is given by

$$H_N' \approx \bar{\Omega}_{rf2} I_2^{x'} + \Omega_{\rm rf1} I_1^x + p g_e' I_1^z I_2^z, \tag{18}$$

in which $\bar{\Omega}_{\rm rf2} = \sqrt{\delta_2^2 + \Omega_{\rm rf2}^2}$. The initial state of the system is $|+_1 -_2\rangle$ and the population (P_+) of the initial state $|+_1\rangle$ of ^{13}C spin is given by

$$P_+ = 1 - \frac{(pg_e' \cos\theta)^2 \sin^2[t\sqrt{(pg_e' \cos\theta)^2 + \Delta^2}/2]}{(pg_e' \cos\theta)^2 + \Delta^2}, \tag{19}$$

where $\cos\theta = \frac{\Omega_{\rm rf2}}{\sqrt{\delta_2^2+\Omega_{\rm rf2}^2}}$ and $\Delta = \bar{\Omega}_{\rm rf2} - \Omega_{\rm rf1}$. The frequency of the rf driving to the ^{29}Si spin is swept to show the detection bandwidth of our method (see Fig. 3). The perfect population transfer could be possible if $|\bar{\Omega}_{\rm rf2} - \Omega_{\rm rf1}| \ll pg_e' \cos\theta$. Namely, the dip position with $\omega_{\rm rf2} = \gamma_{n2}B + \frac{a_{\|2}}{2} = 2\pi \times 5065.5$ kHz indicates $\delta_2 = 0$ and $\Omega_{\rm rf2} = \Omega_{\rm rf1}$. The dip height depends on the longitudinal dipolar coupling with $P_+ = \cos^2(pg_e' T/2)$, with T the total evolution time. Increasing the Rabi frequency of the MW driving induces a smaller effective coupling between the nuclear spins, decreasing the frequency bandwidth (see Fig. 3), which also gives a tunable frequency filter. We investigate the case when there is a third ^{29}Si nuclear spin with coupling $a_{\|3}$ to the NV center and show the efficiency of the selectivity of our scheme. In Fig. 3(b) we initialize the nuclei in the state $|+_1 -_2 -_3\rangle$. We calculate the infidelity of the nuclear ZZ gate between two nuclear spins affected by the third ^{29}Si spin. The first ^{13}C and second silicon spins are coupled to an NV center with $(a_{\|1}, a_{\|2}) = 2\pi \times (11, 9)$ kHz. The coupling of the third spin matches $\delta_3 = (a_{\|2} - a_{\|3})/2 > 2\pi \times 0.5$ kHz, which gives high fidelity of the gate operation of target nuclear spins (greater than 0.95). Thus, our method can address two heteronuclear spins by using the rf fields individually and implement a near-perfect quantum gate at room temperature with high selectivity.

V. SENSING APPLICATION

Another important application of our scheme is to detect nuclear spins in another species outside the diamond. For example, one can use a ^{13}C spin which is well controlled by the NV center to detect ^{1}H spins outside the diamond. Thus ^{13}C spin is initialized in the state $|+_1\rangle$ and ^{1}H spins are in maximally mixed states; one can detect the signal by measuring the probability of the sensor ^{13}C spin remaining in the state $|+_1\rangle$. The related operations are shown in Fig. 2, except for the initialization and readout of ^{1}H spins. To evaluate the effectiveness of our sensing application, we initialize the ^{13}C spin to the state $|+_1\rangle$ to detect the three other nuclear (^{1}H) spins (see Fig. 4). Based on Eq. (19), an rf field is applied to the ^{13}C sensor resonantly and we can adjust the parallel components and control frequency of the rf to match the

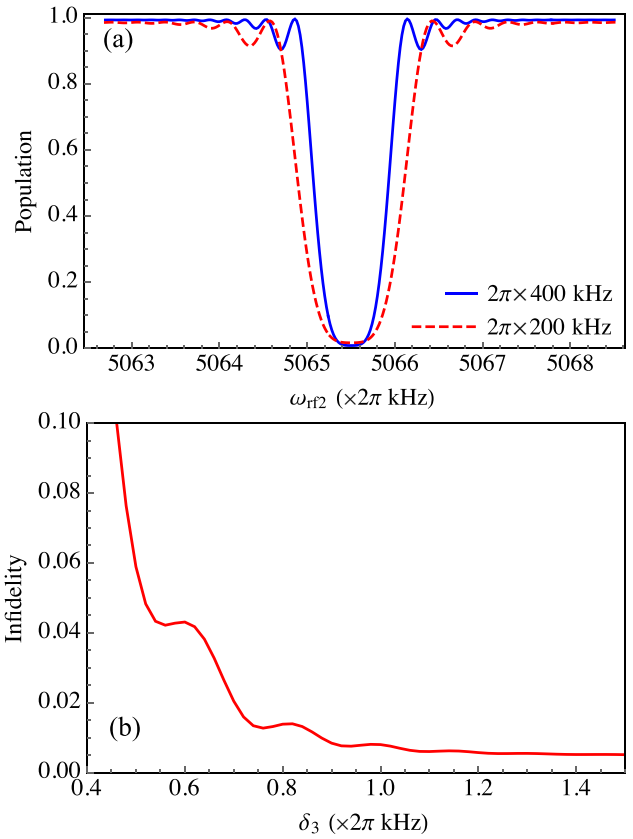

FIG. 3. Numerical simulations for the same parameters as in Fig. 1, i.e., parallel couplings are given as $[a_{\|1}, a_{\|2}] = 2\pi \times (9, 11)$ kHz. (a) Detection bandwidth of the swept rf based on different MW Rabi frequencies. The rf field is applied to the ^{13}C sensor resonantly when the frequency of the other rf field is swept. The evolution time is fixed as $T = (8.8, 4.4)$ ms for $\Omega = 2\pi \times (400, 200)$ kHz. (b) Infidelity of the quantum gate between ^{13}C and ^{29}Si spins when there is another ^{29}Si spin. The infidelity varies with the detuning δ_3, $\delta_3 = (a_{\|3} - a_{\|2})/2$.

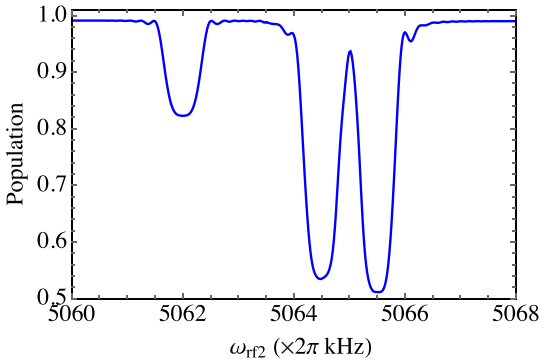

FIG. 4. Assuming one ^{13}C and three ^{1}H spins coupled to the NV center with parallel couplings $(a_{\|1}, a_{\|2}, a_{\|3}, a_{\|4}) = 2\pi \times (11, 4, 9, 11)$ kHz. The ^{13}C spin is the sensor with the initial state $|+_1\rangle$ and the three ^{1}H spins are the targets which are in maximally mixed states. The Larmor frequency for the ^{1}H spins is $\gamma_{n2}B = 2\pi \times 5.06$ MHz. The population of the initial state $|+_1\rangle$ of the ^{13}C sensor is calculated by exact simulation of Eq. (17) with evolution time $T = 8$ ms for $\Omega = 2\pi \times 400$ kHz and the target spin decoherence time $T_2 = 200$ ms.

resonance condition for target (^{1}H) nuclear spins. Once the resonance condition is achieved, the signal dips mark the presence of the nuclear spins. Similar to the case in the previous scheme [29], the frequency resolution is not limited by the NV relaxation $T_{1\rho}$; it requires $|\bar{\Omega}_{\mathrm{rf}i} - \Omega_{\mathrm{rf}1}| > pg'_e \cos\theta$, which is limited by the target spin decoherence time $T_2 = 200$ ms, and the sensitivity per unit time of our scheme is proportional to $pg'_e/\sqrt{1/\Gamma_N} \sim (a_{\parallel i}/4)/\sqrt{T_{1\rho}}$.

VI. CONCLUSION

Before summarizing, we would like to compare our method with the previous scheme [29]. Both schemes realize the effective coupling of target nuclear spins by periodic resetting of electron spins, and the impact of NV decoherence and relaxation processes on these nuclei are suppressed. The difference mainly comes from our employing two weak rf fields to control the heteronuclear spins individually. In the previous approach, nuclear spins in the same species were considered and coarse tuning of the direction of the magnetic field in advance was necessary for matching the resonant condition. Our method allows for effective interaction of nuclear spins in different species, which loosen the requirement of the stringent resonant condition of the previous scheme. The signal accumulation and resonant condition depend on the longitudinal dipolar coupling component $a_{\parallel_i}$, which leads to no information about the transverse coupling component $a_{\perp_i}$ being detected in this scheme. Therefore, less information is detected when one uses this method for sensing nuclear spins near the NV center; however, it also has the advantage that the quantum gate implementation is not limited by the transverse coupling component.

In this work we presented an extension of the dissipatively stabilized NV center to a case in which one achieves a tunable second-order effective coupling between distant nuclear spins in different species. We employed rf fields and MW driving to match the resonant condition and control electron and nuclear spins individually. The coupling is mediated by a dissipatively decoupled electron spin of a NV center, with the impact of NV decoherence and relaxation processes on these nuclei suppressed. Thus the effective indirect interaction enables selective initialization and coherent control of nuclear spins as well as analysis of complex spin structures under ambient conditions.

ACKNOWLEDGMENTS

The authors are grateful for financial support from the Natural Science Foundation of Hunan Province, China (Grant No. 2019JJ10002), Hunan Provincial Hundred People Plan, and Huxiang High-Level Talent Gathering Project (No. 2019RS1043).

[1] T. Taminiau, J. Cramer, T. van der Sar, V. Dobrovitski, and R. Hanson, Nat. Nanotechnol. **9**, 171 (2014).
[2] J. Zhang, S. S. Hegde, and D. Suter, Phys. Rev. A **98**, 042302 (2018).
[3] G. Waldherr, Y. Wang, S. Zaiser, M. Jamali, T. Schulte-Herbrüggen, H. Abe, T. Ohshima, J. Isoya, J. F. Du, P. Neumann, and J. Wrachtrup, Nature (London) **506**, 204 (2014).
[4] L. Robledo, L. Childress, H. Bernien, B. Hensen, P. Alke-made, and R. Hanson, Nature (London) **477**, 574 (2011).
[5] T. H. Taminiau, J. J. T. Wagenaar, T. van der Sar, F. Jelezko, V. V. Dobrovitski, and R. Hanson, Phys. Rev. Lett. **109**, 137602 (2012).
[6] S. Kolkowitz, Q. P. Unterreithmeier, S. D. Bennett, and M. D. Lukin, Phys. Rev. Lett. **109**, 137601 (2012).
[7] N. Zhao, J. Honert, B. Schmid, M. Klas, J. Isoya, M. Markham, D. Twitchen, F. Jelezko, R. B. Liu, H. Fedder, and J. Wrachtrup, Nat. Nanotechnol. **7**, 657 (2012).
[8] A. Ermakova, G. Pramanik, J. M. Cai, G. Algara-Siller, U. Kaiser, T. Weil, Y.-K. Tzeng, H. C. Chang, L. McGuinness, M. Plenio, B. Naydenov, and F. Jelezko, Nano Lett. **13**, 3305 (2013).
[9] H. J. Mamin, M. Kim, M. Sherwood, C. Rettner, K. Ohno, D. Awschalom, and D. Rugar, Science **339**, 557 (2013).
[10] S. Zaiser, T. Rendler, I. Jakobi, T. Wolf, S. Y. Lee, S. Wagner, V. Bergholm, T. Schulte-Herbrüggen, P. Neumann, and J. Wrachtrup, Nat. Commun. **7**, 12279 (2016).
[11] T. Staudacher, F. Shi, S. Pezzagna, J. Meijer, J. Du, C. A. Meriles, F. Reinhard, and J. Wrachtrup, Science **339**, 561 (2013).
[12] M. Pfender, N. Aslam, H. Sumiya, S. Onoda, P. Neumann, J. Isoya, C. A. Meriles, and J. Wrachtrup, Nat. Commun. **8**, 834 (2017).
[13] Y. Wu, F. Jelezko, M. B. Plenio, and T. Weil, Angew. Chem. Int. Ed. **55**, 6586 (2016).
[14] M. Doherty, N. Manson, P. Delaney, F. Jelezko, J. Wrachtrup, and L. Hollenberg, Phys. Rep. **528**, 1 (2013).
[15] D. A. Golter, T. Oo, M. Amezcua, K. A. Stewart, and H. Wang, Phys. Rev. Lett. **116**, 143602 (2016).
[16] D. A. Golter and H. Wang, Phys. Rev. Lett. **112**, 116403 (2014).
[17] J. Casanova, Z. Y. Wang, and M. B. Plenio, Phys. Rev. Lett. **117**, 130502 (2016).
[18] A. Bermúdez, F. Jelezko, M. B. Plenio, and A. Retzker, Phys. Rev. Lett. **107**, 150503 (2011).
[19] J. Zimmermann, P. London, Y. Yirmiyahu, F. Jelezko, A. Blank, and D. Gershoni, Phys. Rev. B **102**, 245408 (2020).
[20] X. Rong, J. Geng, Z. Wang, Q. Zhang, C. Ju, F. Shi, C. K. Duan, and J. Du, Phys. Rev. Lett. **112**, 050503 (2014).
[21] S. S. Hegde, J. Zhang, and D. Suter, Phys. Rev. Lett. **124**, 220501 (2020).
[22] M. Abobeih, J. Randall, C. Bradley, H. Bartling, M. Bakker, M. Degen, M. Markham, D. Twitchen, and T. Taminiau, Nature (London) **576**, 411 (2019).
[23] C. E. Bradley, J. Randall, M. H. Abobeih, R. C. Berrevoets, M. J. Degen, M. A. Bakker, M. Markham, D. J. Twitchen, and T. H. Taminiau, Phys. Rev. X **9**, 031045 (2019).
[24] Z. Y. Wang, J. Casanova, and M. Plenio, Nat. Commun. **8**, 14660 (2017).

[25] B. Tratzmiller, J. F. Haase, Z. Wang, and M. B. Plenio, Phys. Rev. A **103**, 012607 (2021).
[26] J. Casanova, Z.-Y. Wang, and M. B. Plenio, Phys. Rev. A **96**, 032314 (2017).
[27] M. Degen, S. Loenen, H. Bartling, C. Bradley, A. Meinsma, M. Markham, D. Twitchen, and T. Taminiau, Nat. Commun. **12**, 3470 (2021).
[28] J. Bian, M. Jiang, J. Cui, X. Liu, B. Chen, Y. Ji, B. Zhang, J. Blanchard, X. Peng, and J. Du, Phys. Rev. A **95**, 052342 (2017).
[29] Q. Chen, I. Schwarz, and M. B. Plenio, Phys. Rev. Lett. **119**, 010801 (2017).
[30] S. L. Bayliss, D. W. Laorenza, P. J. Mintun, B. D. Kovos, D. E. Freedman, and D. D. Awschalom, Science **370**, 1309 (2020).
[31] J. Cai, A. Retzker, F. Jelezko, and M. B. Plenio, Nat. Phys. **9**, 168 (2013).
[32] M. Radulaski, M. Widmann, M. Niethammer, J. L. Zhang, S. Y. Lee, T. Rendler, K. G. Lagoudakis, N. T. Son, E. Janzen, T. Ohshima, J. Wrachtrup, and J. Vuckovic, Nano Lett. **17**, 1782 (2017).
[33] E. M. Kessler, Phys. Rev. A **86**, 012126 (2012).
[34] S. Bravyi, D. DiVincenzo, and D. Loss, Ann. Phys. (NY) **326**, 2793 (2011).
[35] R. Hanson, V. V. Dobrovitski, A. E. Feiguin, O. Gywat, and D. D. Awschalom, Science **320**, 352 (2008).
[36] C. Lei, S. J. Peng, C. Y. Ju, M. H. Yung, and J. F. Du, Sci. Rep. **7**, 11937 (2017).
[37] F. Reiter and A. S. Sørensen, Phys. Rev. A **85**, 032111 (2012).
[38] F. Jelezko, I. Popa, A. Gruber, C. Tietz, J. Wrachtrup, A. Nizovtsev, and S. Kilin, Appl. Phys. Lett. **81**, 2160 (2002).
[39] F. Jelezko, T. Gaebel, I. Popa, A. Gruber, and J. Wrachtrup, Phys. Rev. Lett. **92**, 076401 (2004).
[40] P. Neumann, J. Beck, M. Steiner, F. Rempp, H. Fedder, P. Hemmer, J. Wrachtrup, and F. Jelezko, Science **329**, 542 (2010).
[41] J. Cai, F. Jelezko, M. B. Plenio, and A. Retzker, New J. Phys. **15**, 013020 (2013).